Self-Aligning Exoskeleton Hip Joint: Kinematic Design with Five Revolute, Three Prismatic and One Ball Joint

Jonas Beil, Charlotte Marquardt and Tamim Asfour

***Abstract*— Kinematic compatibility is of paramount importance in wearable robotic and exoskeleton design. Misalignments between exoskeletons and anatomical joints of the human body result in interaction forces which make wearing the exoskeleton uncomfortable and even dangerous for the human. In this paper we present a kinematically compatible design of an exoskeleton hip to reduce kinematic incompatibilities, so called macro- and micro-misalignments, between the human's and exoskeleton's joint axes, which are caused by inter-subject variability and articulation. The resulting design consists of five revolute, three prismatic and one ball joint. Design parameters such as range of motion and joint velocities are calculated based on the analysis of human motion data acquired by motion capture systems. We show that the resulting design is capable of self-aligning to the human hip joint in all three anatomical planes during operation and can be adapted along the dorsoventral and mediolateral axis prior to operation. Calculation of the forward kinematics and FEM-simulation considering kinematic and musculoskeletal constraints proved sufficient mobility and stiffness of the system regarding the range of motion, angular velocity and torque admissibility needed to provide $50\,\%$ assistance for an $80\,\mathrm{kg}$ person.**

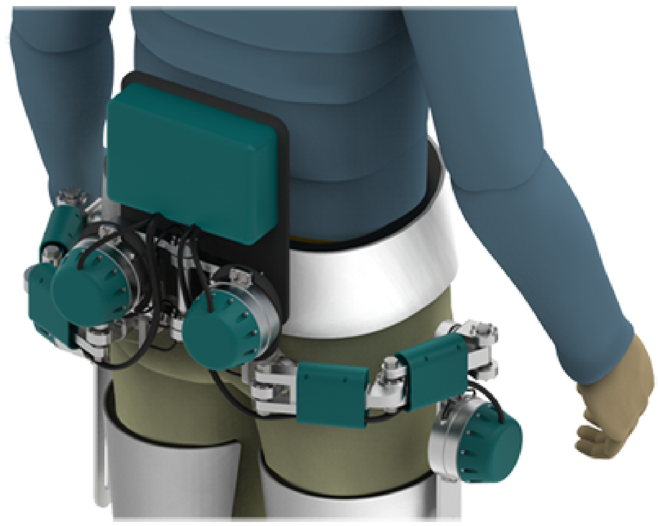

Fig. 1. A rendering of the hip exoskeleton prototype.

I. INTRODUCTION

In wearable robotics, considerable research efforts are directed at the design and development of exoskeletons, which fulfill the major requirement of comfortable and safe wearability by a human user. Such fundamental requirements are the key for increasing the user acceptance and achieving efficient augmentation of user capabilities. The inter-subject variability of the human musculoskeletal system, articulation and soft tissue deformation make it challenging to build wearable robots such as exoskeletons, whose joint axes are in continuous alignment with joint axes of the the human body. Kinematic incompatibilities, macro- or micro-misalignments between the instantaneous center of rotation (ICR) of the axes of user and exoskeleton are the cause of discomfort or even pain of the user and can impair the correct execution of training motions or motion sequences at work [1]. In this paper, we address the problem of the design of a kinematically compatible exoskeleton hip joint.

Alignment of the hip joint is very important for the design of lower limb exoskeletons. Non-anthropomorphic kinematics including supplementary joints to decrease macro- and micro-misalignments have been proposed as a promising way for avoiding the misalignment problem. Misalignments at the hip propagate to the knee and ankle joint or vice versa. The structure of the human hip joint as a ball joint with three degrees of freedom (DOF) prevents an exoskeleton design with technically equivalent solution to align the ICRs of all joint axes.

Macro-misalignments occur if the exoskeleton's DOF differ from the DOFs of the human. If the joints are oversimplified, either the exoskeleton structure between the DOFs can not be aligned to the human's segment lengths or the range of motion (ROM) of the exoskeleton is less than the human one [2]. Exoskeleton designs like the Mindwalker exoskeleton [3], the XOR2 [4] or the lower body exoskeleton presented in [5] use three revolute joints to represent the three DOF in the hip, accepting misalignments to keep the design simple.

To adjust the exoskeleton to the inter-subject variability, manual adaptable mechanism like clamping mechanisms [6] or screws ([3], [7]) were integrated in these designs, as well as, different frame sizes [8] to regulate the link length. Further comfort improvements are achieved by adding passive DOF between the physical human robot interface (pHRI) and the exoskeleton, like a sliding and rotational adjustment to an orthotic shell for an assistive hip orthosis [9] or supplementary joints to self-align the wrist and forearm joints [10].

Micro-misalignments are mainly caused by the complexity of the musculoskeletal system resulting in non-coincident

This work has been supported by the German Federal Ministry of Education and Research (BMBF) under the project INOPRO.

The authors are with the High Performance Humanoid Technologies Lab (H^2T), Institute for Anthropomatics and Robotics, Karlsruhe Institute of Technology (KIT), Germany, {jonas.beil, asfour}@kit.edu charlotte.marquardt@student.kit.edu

joint rotation axes between the exoskeleton and the user [2]. The IHMC mobility assist exoskeleton [11] or the BLERE [12] incorporate curved bearings representing the yaw axis between two revolute joints to reduce the misalignment. In our previous work, we developed an hip mechanism for a lower limb exoskeleton using two prismatic and three revolute joints which self-align to the user's hip yaw axis in the transverse plane [13].

This paper presents the further development of the aforementioned hip exoskeleton using supplementary joints to reduce macro- and micro-misalignments in all three anatomical planes and can be integrated in an exoskeleton for the lower extremities. We propose a combination of revolute, prismatic and ball joints for the online alignment (during operation) of the exoskeleton in the transverse, frontal and sagittal plane as well as mechanism for the offline adaption (prior to operation) to the subject on the dorsoventral and mediolateral axis.

The paper is structured as follows. Section II describes the requirements for the system derived from human hip anatomy, human motion analysis and the chosen kinematics as well as the construction and actuation of the device. Theoretical evaluation of the design using the forward kinematics to calculate the maximum joint angles considering kinematic and anatomic constraints is presented in Section III. Section IV concludes the paper.

II. Design of the Hip Exoskeleton

A. Requirements

The human hip joint is a ball and socket joint which allows rotational movement describable in the sagittal, frontal and transverse plane. Additional translational movement in the joint is minimized by tendons and ligaments, as well as the bone structure [14]. Although the translational movements are very small, an exoskeleton should be flexible in order to compensate differences in body characteristics and differences occurring through changes in the body posture, e.g. the change of hip width when sitting and standing.

The 5th to 95th percentile of hip width of adults aged between 18 to 65 years when standing is $325 \cdots 400\,\mathrm{mm}$ and increases to $350 \cdots 470\,\mathrm{mm}$ when sitting. This correlates with body sizes between $1.535 \cdots 1.855\,\mathrm{m}$ for men and women, according to the German DIN-Norm [15]. Since a construction covering the full range of body sizes and hip widths would be complex and possibly a trade-off between size and ROM of the joints, four exoskeleton sizes (XS-L) were defined by dividing the range of body height in four consistent segments.

According to [14], the human hip allows maximum extension and flexion (E/F) motions up to -20$\cdots$120° in the sagittal plane, -25$\cdots$40° of adduction and abduction motion (Add/Abd) in the frontal plane and and internal and external rotation (IR/ER) of -35$\cdots$45° in the transverse plane. In [13], we already investigated joint angles and joint velocities during activities of daily living. In this work a data set including 828 Motions of 26 subjects from motion recordings available in the KIT Whole-Body Human Motion Database[1] were analyzed [16]. The determined ROMs and joint velocities based on this analysis are given in Table I.

TABLE I
REQUIRED ROM AND JOINT VELOCITIES FROM [13]

Joint	ROM [°]	Joint vel. [rad/s]
Add/Abd	$-8.8 \cdots 13.4$	$-1.14 \cdots 0.93$
IR/ER	$-10.5 \cdots 13.6$	$-1.85 \cdots 1.73$
E/F	$-14.8 \cdots 100$	$-2.8 \cdots 3.75$

For the design of the exoskeleton, the hip joint mechanism should be able to realize ROMs and angular velocities derived from the analysis to avoid macro-misalignments when reaching the joint limits or discomfort when moving slower than the natural moving speed of the user.

In addition, we envision an assistance rate of $50\,\%$ for an $80\,\mathrm{kg}$ user (50th percentile of body weight for males [15]) walking forward. According to [14] the maximum hip torque in the sagittal plane occurs at $10\,\%$ of gait cycle and is $1.2\,\mathrm{Nm/kg}$, which leads to a maximum actuator torque of $48\,\mathrm{Nm}$. In the frontal plane the maximum hip torque of $1.1\,\mathrm{Nm/kg}$ at $12\,\%$ of gait cycle results in a maximum actuator torque of $44\,\mathrm{Nm}$ for the roll joint. Torque in the transverse plane is relatively low $(0.2\,\mathrm{Nm/kg})$ compared to the aforementioned two, so we believe that actuation of this axis is not essentially needed. Energy storing elements like parallel springs could be sufficient to support the user.

B. Kinematics

A ball joint can be modelled by using one revolute joint for every spatial direction if their joint axes intersect in one point. Regarding human anatomy this is only possible in the sagittal (pitch axis) and frontal plane (roll axis) but not in the transverse plane (yaw axis) if the kinematic chain is situated outside of the human body.

However, the movement in the sagittal and frontal plane depends on the rotational movement of the hip. Therefore the exoskeleton requires a structure that allows rotating the pitch and roll axis around the yaw axis. Simultaneously the exoskeleton is supposed to be adjustable to varying body sizes. As the inter-subject variability of the human musculoskeletal system does not allow a rigid circular solution such as a rail, we propose a structure of redundant joints.

Initially occurring macro-misalignments after donning the exoskeleton can be avoided by an offline alignment of the roll axis in the dorsoventral and mediolateral axis, resulting simultaneously in an offline alignment of the pitch and yaw axis. Further macro- and micro-misalignments in the transverse plane can be minimized through a self-aligning mechanism.

In our design concept, we assume that the shape of one half of the pelvis can be modeled by an ellipse with the radii r_{AA} and r_{FE}, indicated by the dashed line in Fig. 2. Furthermore, we presume the difference between both radii averages around $30\,\mathrm{mm}$. To realize a circular movement

[1] https://motion-database.humanoids.kit.edu/

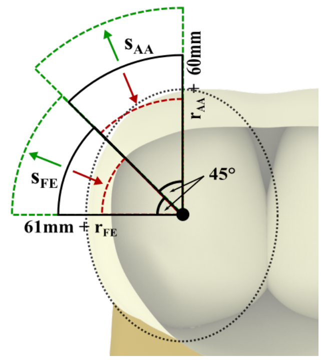

Fig. 2. Top view on the modeled shape of the hip and the two circle segments forming the ellipse around the center of the hip.

around the hip center, the kinematic chain is designed along the chords of the $45°$ segments of the circles with the radii $r_{AA} + 60\,\mathrm{mm}$ and $r_{FE} + 61\,\mathrm{mm}$, as shown in Fig. 2.

Consequently we developed a conceptual design which consists of a prismatic and a revolute joint for the yaw axis, one ball joint for the roll axis, one revolute joint for the pitch axis and a combination of revolute and prismatic joints between the roll and pitch axis along the chords of the two circles to increase adaptability. By positioning the yaw mechanism prior to the roll and pitch joint a simultaneous rotational movement and alignment of both axes in the transverse plane around the hip center is assured (Fig. 3). If a movement around the yaw axis is followed by a movement around the roll axis, all joint axes persist coaxial. In case a movement around the roll axis is followed by a movement around the yaw axis, the roll and pitch axis do not remain orthogonal, but the ICR of human hip and exoskeleton still coincide.

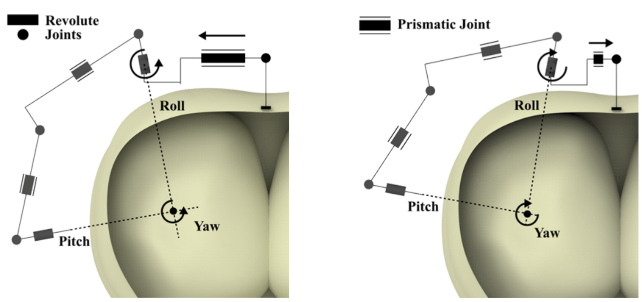

Fig. 3. Top view on the schematic model of the aligned yaw mechanism during $-5°$ internal (left) and $5°$ external (right) rotation.

Fig. 5 shows a schematic representation of the kinematics, described by standard Denavit-Hartenberg (DH) parameters, which are given in Table II. The base (B) of the chain is positioned at the middle of the users back on the part holding the electronic components. Table III presents the joints and their range of motion. The parameter o_i is introduced to describe an offset which can be adjusted before wearing the exoskeleton, while θ_i and d_i define the angle or the displacement of an revolute or prismatic joint during operation.

The roll axis can be adjusted offline through an offset o_1 in vertical direction by a screw at the connection between the belt and the base of the kinematic chain B by $\pm 20\,\mathrm{mm}$ (Fig. 4, right). Additional offline alignment through an offset o_3 in the horizontal direction with a screw at the shaft of the joint by $\pm 10\,\mathrm{mm}$ is possible (Fig. 4, left). If further adjustment is required the roll axis can self align through the prismatic joint of the yaw axis (d_3) at the user's back. The end of the chain is marked by the part designed to connect the device to the users thigh, which is adjustable offline through offset o_{12}.

TABLE II

DH PARAMETERS OF THE HIP DESIGN FOR THE MANIKIN

i	Angle θ_i	Disp d_i	Length a_i	Twist α_i
1	0	o_1	49.64	0
2	θ_2	0	0	-90
3	95.46	$99 + o_3 + d_3$	85.39	0
4	95.46	0	0	90
5	$90 + \theta_5$	0	0	90
6	$180 + \theta_6$	31.5	0	90
7	$-112.5 + \theta_7$	0	0	-90
8	0	$137.77 + d_8$	27.72	90
9	$-45 + \theta_9$	0	0	-90
10	0	$114.52 + d_{10}$	0	90
11	$67.5 + \theta_{11}$	0	0	90
12	$90 + \theta_{12}$	55.89	$260 + o_{12}$	-90

TABLE III

RANGE AND TYPE OF ALIGNING MECHANISM FOR THE MANIKIN

Parameter	Type	Mode	Adjustment	Stroke/Angle
o_1	offset	passive	offline	$\pm 20\,\mathrm{mm}$
θ_2	revolute	passive	online	$0 \cdots 14.5°$
o_3	offset	passive	offline	$\pm 10\,\mathrm{mm}$
d_3	prismatic	passive	online	$\pm 25\,\mathrm{mm}$
θ_5	revolute	passive	online	$\pm 15°$
θ_6	revolute	active	online	*roll angles*
θ_7	revolute	passive	online	$-2.5 \cdots 22.5°$
d_8	prismatic	passive	online	$\pm 6.25\,\mathrm{mm}$
θ_9	revolute	passive	online	$-15 \cdots 25°$
d_{10}	prismatic	passive	online	$\pm 6.25\,\mathrm{mm}$
θ_{11}	revolute	passive	online	$-2.5 \cdots 22.5°$
θ_{12}	revolute	active	online	*pitch angles*
o_{12}	offset	passive	offline	$\pm 50\,\mathrm{mm}$

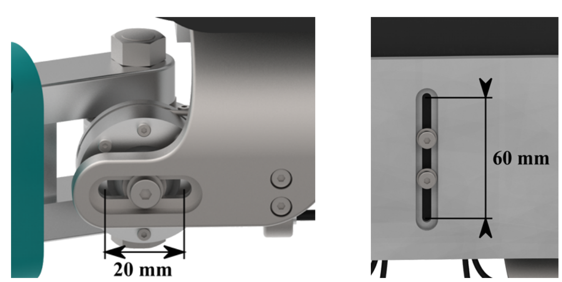

Fig. 4. Detailed view on the offline adaptability of the roll axis in horizontal (o_1, left) and vertical (o_3, right) direction.

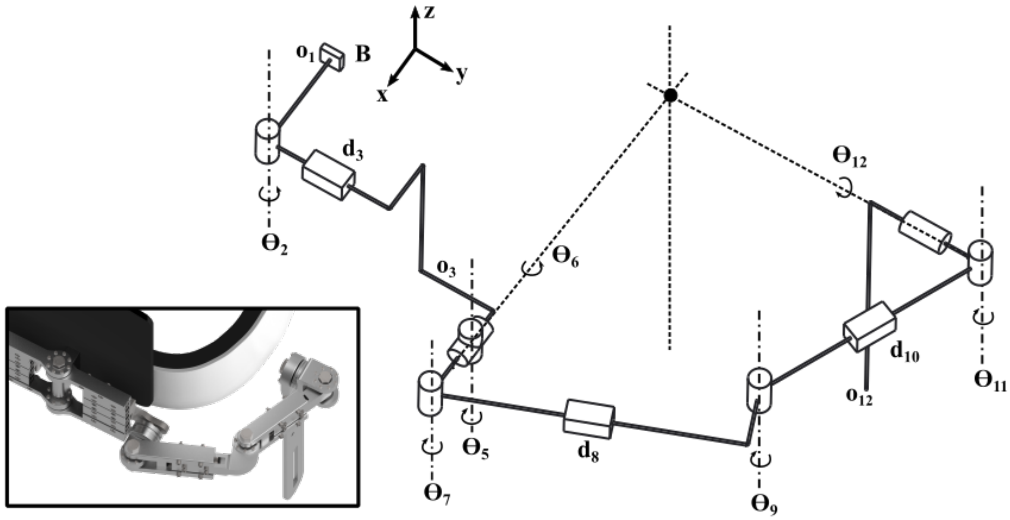

Fig. 5. Schematic model of the kinematic structure with the corresponding DH-parameter (d_i, θ_i) and offsets (o_i).

To achieve the maximum possible range of motion for the yaw joint (d_3), two precision rail guides (LWRE 3050, SKF GmbH) are combined to allow a stroke of $\pm 25\,\mathrm{mm}$. Due to the low maximum torques and power, we did not consider actuating this joint. However, parallel elastic elements connecting the two parts of the prismatic joints are integrated to offer a small support while moving. Moreover, the springs allow the prismatic joints to move back to their neutral position.

As a basis for the actuated roll joint (θ_6, Fig. 4, right), a radial ball joint bearing (GEH 10 C, SKF GmbH) with tilting angles up to $15°$ was chosen to allow self-alignment of the roll axis. Although the rotation of this joint around the axis parallel to the sagittal plane is not required, the ball joint uses only a small installation space and an oval shaft is restricting the motion in this direction. The basis for the actuated pitch joint (θ_{12}, Fig. 4, left) consists of a grooved ball bearing (6200-2Z, SKF GmbH) allowing a support of loads resulting from an $80\,\mathrm{kg}$ user.

To adjust the size of the exoskeleton, it could be considered to shorten the parts holding the prismatic joints d_8 and d_{10} and the yaw-roll-connector (Fig. 7) by approximately $5\,\mathrm{mm}$ for each size.

The interfaces at the hip and thigh consist of an outer synthetic hard-shell and an orthopedic inlet. Velcro straps at the front of the thigh and a belt at the hip should allow a comfortable fit.

C. Actuation

As stated before, the highest maximum torques and joint velocities occur in the roll (θ_6) and pitch (θ_{12}) joints. These two joints are actuated by the actuator developed in our group and presented in [17], which is modified for the usage in exoskeletons. It basically consists of a brushless DC-motor coupled to a Harmonic Drive gear and incorporates relative position encoding at the drive side, as well as, absolute position encoding at the link side.

Originally designed for the use in humanoid robots, the unit includes all electronics for motor control, an EtherCAT interface, a hollow shaft, an inertial measurement unit and an output torque sensor into its housing which increases the length and diameter of the unit. To realize a compact actuator all electronics are now positioned outside of the unit at the user's back (Fig. 7).

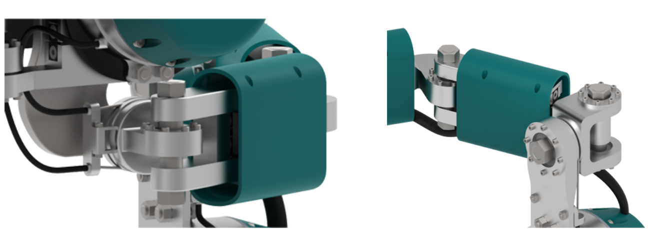

Fig. 6. Detailed view on the two actuated joints in frontal (θ_6, left) and sagittal (θ_{12}, right) plane.

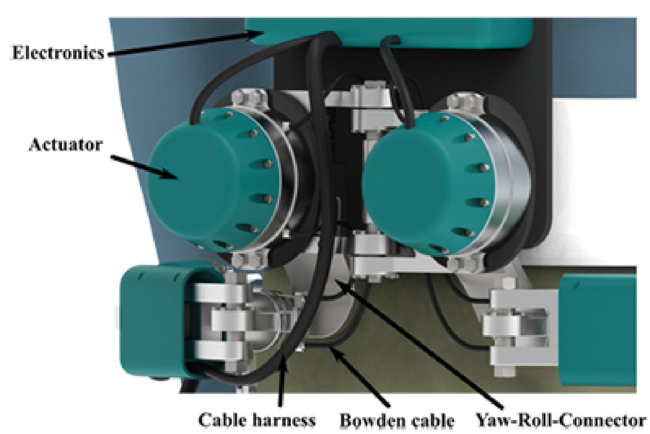

Fig. 7. Back view on the actuation unit for the roll axis and the electronics unit.

The electronic cables for each side of the exoskeleton are merged into one cable harness per side and pass through between both actuators at the back of the exoskeleton. A cable channel in the bottom of the cases (Fig. 7) around the prismatic joints d_8 and d_{10} for the cables prevents them to interfere with the kinematic chain or the user.

Torque transmission is realized by $1.5\,\mathrm{mm}$ steel cables which are connected to cable pulleys with a diameter of $40\,\mathrm{mm}$ at the actuator and $30\,\mathrm{mm}$ at the joints. As the actuator is not positioned directly above the cable pulleys, the steel cables are led by stiff bowden cables to avoid a restriction of the yaw mechanism (Fig. 7).

At the roll axis the bowden cables are mounted directly around the radial ball joint (Fig. 6, left). A gliding ring assures that the mounting part of the bowden cables stays in a vertical position during a rotational movement. Nevertheless, the bowden cables are able to move when the roll joint is tilted to align the axes and ensure that the point of application of the torque remains always in the middle of the ball joint.

With a maximum actuator torque of $64\,\mathrm{Nm}$ at $3.1\,\mathrm{rad/s}$, the maximum joint torque is $48\,\mathrm{Nm}$ at a maximum velocity of $4.1\,\mathrm{rad/s}$. Instead of using a hollow shaft and strain gauges to measure actuator torques, one load cell (FMT6, TE Connectivity Ltd.) is positioned at the mounting point of the cables in a hollow space within the actuator to measure the tensile forces in the steel cables. This reduces the actuator length to $55\,\mathrm{mm}$ and the maximum outer diameter to $88\,\mathrm{mm}$.

III. Evaluation and Results

To prove the adaptability, sufficient mobility and load capacity of the exoskeleton, the evaluation of the design is separated in three steps. Section III-A describes the calculation of the range of body heights for which each exoskeleton size can be worn. This is necessary to determine the range of motion per exoskeleton size and body height, which is described in III-B. Section III-C concludes with the actuation and torque admissibility of the exoskeleton.

A. Exoskeleton sizes

The exoskeleton was initially designed for a manikin offered by PTC Creo (PTC Inc, Needham, USA) and fulfills the H-ANIM Standards of the ISO/IEC 19774 [18].

To produce comparable results, the evaluation of the exoskeleton sizes and corresponding body proportions is based on the generalized assumption of Winter [19], where not only the distance between the hip centers but also the hip width depends on the body height.

According to this assumption the outer hip width is $19.1\,\%$ of the body height. Previous Winter based work presented in [20] states the distance between the hip centers to be $10.4\,\%$ of the body height leading to a hip radius at the pitch joint r_{FE} of $4.35\,\%$ and at the roll joint r_{AA} (equal to hip depth) of $6.49\,\%$ per body height.

Stroke variation of the prismatic joints d_8 and d_{10} results in ellipse radii r_{FE} and r_{AA} (Fig. 2) between $81\cdots 97\,\mathrm{mm}$ at the pitch axis and between $112\cdots 128\,\mathrm{mm}$ at the roll axis. This can be calculated using Eq. 1, where s_{AA} and s_{FE} present the length of the chords of the $45°$ segments of the circles.

$$\begin{aligned} r_{AA} &= \frac{s_{AA}}{2\cdot sin\left(\frac{\pi}{8}\right)} - 60\,\mathrm{mm} \\ r_{FE} &= \frac{s_{FE}}{2\cdot sin\left(\frac{\pi}{8}\right)} - 61\,\mathrm{mm} \end{aligned} \tag{1}$$

Using the aforementioned correlations, the actual design would allow users with body heights ranging from $1.88\cdots 2.14\,\mathrm{m}$ to wear the exoskeleton. As these values exceed the required body heights derived from the DIN-Norm, a fifth exoskeleton size (XL) is added.

To reach the required sizes of the DIN-Norm, the parts holding the prismatic joints d_8 and d_{10} and the yaw-roll-connector (Fig. 7) have to be shortened by $3\,\mathrm{mm}\cdots 5\,\mathrm{mm}$ for each size. If the relation between body height and corresponding hip width is not compatible for the user, the yaw-roll-connector can be combined with a different length of the parts holding the prismatic joints.

The required sitting volume of the exoskeleton is measured from the outer shell of the body amounts to $137\,\mathrm{mm}$ in dorsal and $89\,\mathrm{mm}$ in lateral direction. Presuming that the distance between the transverse plane of the hip joint and the human sitting plane will not fall below a distance of $35\,\mathrm{mm}$ with the reduction of the human body height, the exoskeleton allows sitting without slipping in cranial direction.

The increasing hip width while sitting can be compensated due to the possibility of self-adjustment of the three prismatic joints d_3, d_8 and d_{10} to the exoskeleton width during operation . That is the reason why this is not considered for calculating the ROMs.

TABLE IV
Exoskeleton sizes with regard to yaw mechanism

Size	Body heights [m]	Hip width [mm]
XS	$1.44\cdots 1.63$	$258\cdots 311$
S	$1.55\cdots 1.74$	$283\cdots 339$
M	$1.66\cdots 1.89$	$307\cdots 368$
L	$1.77\cdots 2.01$	$332\cdots 393$
XL	$1.87\cdots 2.11$	$356\cdots 417$

B. Range of Motion

Calculations of the ROM for the yaw joint is based on geometric correlations with regard to the constraints mentioned in Table III and to the schematic model in Fig. 3. The yaw angles for each exoskeleton size are calculated with respect to the maximum tilting angle of the roll joint. This tilting angle also increases the ellipse radii r_{FE} and r_{AA} by Δr_{FE} and Δr_{AA} respectively. Table IV presents the resulting body heights and the corresponding hip widths and Fig. 8 shows the average yaw joint angles for each body height.

If the yaw joint angle exceeds $\pm 9.8°$, the prismatic joint d_3 is fully extended and the joints d_8 and d_{10} fulfill the function of the yaw mechanism. This leads to a misaligned roll axis,

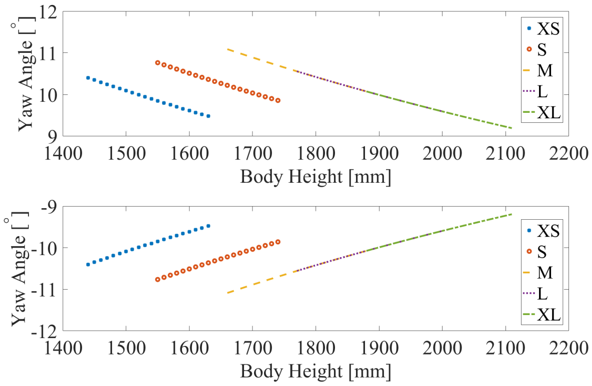

Fig. 8. Maximum (top) and minimum (bottom) yaw angles with alignment in all three anatomical planes.

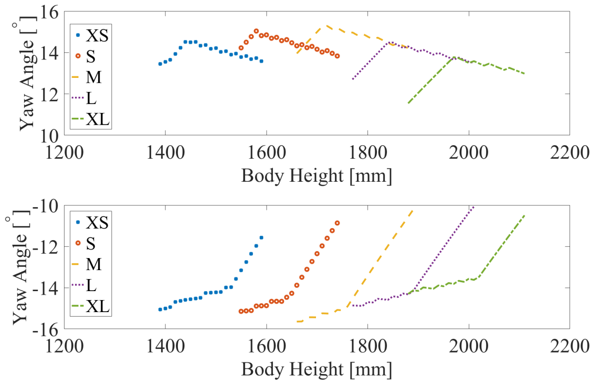

Fig. 10. Maximum (top) and minimum (bottom) yaw angles considering a small misalignment of the roll axis.

which is considered in Eq. 2 to calculate the maximum and minimum yaw joint angles with this assumption. In Fig. 10 the resulting maximum misaligned internal and external angles are shown.

$$\begin{aligned}\delta_{AA} &= 2 \cdot asin\left(\frac{s_{AA}}{2 \cdot (r_{AA} + \Delta r_{AA} + 60\,\mathrm{mm})}\right) - \frac{\pi}{4} \\ \delta_{FE} &= 2 \cdot asin\left(\frac{s_{FE}}{2 \cdot (r_{FE} + \Delta r_{FE} + 61\,\mathrm{mm})}\right) - \frac{\pi}{4}\end{aligned} \tag{2}$$

Comparing this with the aforementioned analysis, we can reach the conclusion that the exoskeleton can self align during most activities. Yaw angles exceeding $\pm 9.8°$ will result in a maximum roll axis deviation of $-0.7 \cdots 3.8°$. From this follows that $72 \cdots 93\,\%$ of the required yaw angles can be reached without roll axis deviation and $93\,\%$ with deviation.

The adduction angle is also only restricted by the mounting point of the steel cable. To cover the required angle as well as a small safety addition a maximum of $20°$ was chosen. The distance between the hip centers (resulting in a change of o_3) and the yaw angle influence the angle of abduction (Fig. 6, left), as it is restricted by the horizontal distance to the actuator. Fig. 9 shows the average possible roll angle per body height. The abduction angle first equals the required angle of $13.4°$ at $1.58\,\mathrm{m}$. From this follows that $95\,\%$ of the subjects covered by the DIN-Norm can wear the exoskeleton.

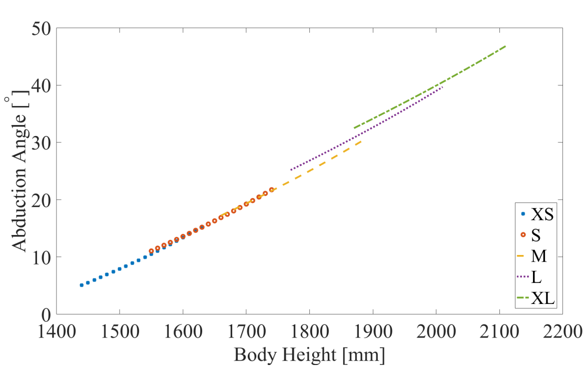

Fig. 9. Maximum abduction angles per body height.

In the sagittal plane, the flexion angle is only restricted by the mounting point of the steel cable. To allow sitting, we have chosen a maximum flexion angle of $120°$. Considering a collision-free movement the extension angle is restricted by the serial chain prior to this axis and can reach up to $31.35°$ (Fig. 6, right).

C. Actuation

The cable pulley in the actuator was designed that the maximum actuator torque equates to the maximum required torque for the pitch joint ($48\,\mathrm{Nm}$). The resulting angular velocities exceed the requirements by $2.96\,\mathrm{rad/s}$ in the roll and by $0.35\,\mathrm{rad/s}$ in the pitch axis.

Torque admissibility of the exoskeleton is examined with FEM-Analysis, acting on the assumption that every part is made of Aluminium 7050. We prove the torque admissibility for the case where the users prevents exoskeleton movement while maximum torque is exerted by the actuators. Due to the back driveability a torque higher than the maximum torque of the actuator will lead to actuator motion. This is modeled by exerting $44\,\mathrm{Nm}$ at the mounting point of the roll joint and $48\,\mathrm{Nm}$ at the mounting point of the the pitch joint corresponding to the maximum joint torque. The resulting maximum Von Mises stress is $365\,\mathrm{MPa}$ with a displacement of $12.69\,\mathrm{mm}$, which affects mostly the shafts and the yaw-roll-connector (Fig. 11). Therefore the yaw-roll-connector and the shafts will be produced of steel and the remaining parts will be produced of aluminum or carbon fiber. This results in an approximate total weight of $5.0\,\mathrm{kg}$.

IV. Conclusions and Future Work

We presented the design of a hip exoskeleton which is able to self-align to inter-subject characteristics in all three anatomical planes reducing macro- and micro-misalignments while wearing the exoskeleton and during operation. The requirements regarding body height and hip width were derived from the DIN-Norm, while the necessary ROM and

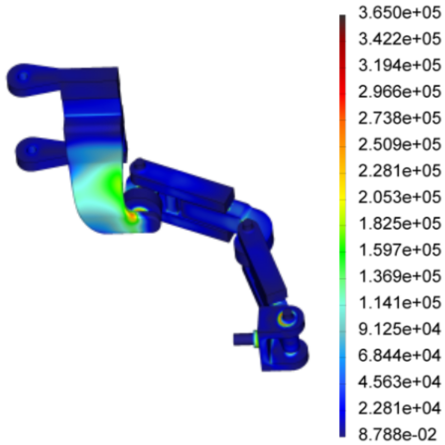

Fig. 11. FEM results of Von Mises stress for Aluminium 7050 in kPa.

joint velocities were gathered by human motion experiments conducted in our previous works. Our design consists of a chain of three prismatic, five revolute and one ball joint for online alignment of the device and three mechanisms to allow offline adjustments to the subject. The roll and pitch joints are actuated by rotational actuators using steel cables for torque transmission and including torque measurement as well as relative and absolute position encoding.

The structure of the exoskeleton allows adjustment of the parts resulting in a $100\,\%$ coverage of the required body heights from the DIN-Norm. Calculation of the forward kinematics proved sufficient mobility of the system to achieve the specified the joint angles and angular velocities of all three hip joints for $95\,\%$ of the body heights. Further, simulations also indicated that the structure should be rigid enough to admit torques required to enable $50\,\%$ assistance for an $80\,\mathrm{kg}$ person.

Based on these promising results, we will conduct an experimental evaluation with a prototype in the near future. This prototype will have the ability to lock single joints to study the effect of the proposed mechanisms to adjust the exoskeleton to the user. Force sensors to measure the interaction forces between the user and the exoskeleton will be integrated and used to asses the increase or decrease on user comfort due to adding or removing single joints of the exoskeleton.

References

[1] A. Schiele, *Fundamentals of ergonomic exoskeleton robots*. Delft University of Technology, 2008.
[2] J. Pons, *Wearable Robots: Biomechatronic Exoskeletons*. Wiley, 2008.
[3] S. Wang and H. van der Kooij, “Modeling, Design, and Optimization of Mindwalker Series Elastic Joint,” in *2013 IEEE International Conference on Rehabilitation Robotics June 24-26, 2013 Seattle, Washington USA*. IEEE, 2013.
[4] S.-H. Hyon *et al.*, “Design of hybrid drive exoskeleton robot XoR2,” in *2013 IEEE/RSJ International Conference on Intelligent Robots and Systems (IROS)*, Nov 2013, pp. 4642–4648.
[5] N. Costa and D. G. Caldwell, “Control of a biomimetic ”soft-actuated” 10dof lower body exoskeleton,” in *The First IEEE/RAS-EMBS International Conference on Biomedical Robotics and Biomechatronics, 2006. BioRob 2006*. IEEE, 2006, pp. 495–501.
[6] EKSO bionics Website (2017). [Online]. Available: www.eksobionics.com
[7] ReWalk Robotics GmbH Website (2017). [Online]. Available: http://rewalk.com/
[8] CYBERDYNE Inc. HAL Website (2017). [Online]. Available: www.cyberdyne.jp
[9] F. Giovacchini *et al.*, “A light-weight active orthosis for hip movement assistance,” *Robotics and Autonomous Systems*, vol. 73, pp. 123–134, 2015.
[10] H. van der Kooij, “Design of a self-aligning 3-DOF actuated exoskeleton for diagnosis and training of wrist and forearm after stroke,” in *International Conference on Rehabilitation Robotics*, 2013.
[11] H. K. Kwa *et al.*, “Development of the IHMC Mobility Assist Exoskeleton,” in *2 009 IEEE International Conference on Robotics and Automation Kobe International Conference Center Kobe, Japan, May 12-17, 2009*. IEEE, 2009.
[12] W. Yang *et al.*, “Design of an Anthropomorphic Lower Extremity Exoskeleton with Compatible Joints,” in *Proceedings of the 2014 IEEE International Conference on Robotics and Biomimetics*. IEEE, 2014.
[13] J. Beil and T. Asfour, “New Mechanism for a 3 DOF Exoskeleton Hip Joint With Five Revolute and Two Prismatic Joints,” in *2016 6th IEEE International Conference on Biomedical Robotics and Biomechatronics (BioRob)*, June 2016, pp. 787–792.
[14] D. A. Neumann, *Kinesiology of the musculoskeletal system: foundations for rehabilitation*. Elsevier Health Sciences, 2013.
[15] “Din 33402-2 (2005-12): Ergonomics - human body dimensions - part 2: Values,” Dec. 2005.
[16] C. Mandery *et al.*, “The KIT Whole-Body Human Motion Database,” in *International Conference on Advanced Robotics (ICAR)*, July 2015, pp. 329–336.
[17] S. Rader *et al.*, “Design of a High-Performance Humanoid Dual Arm System with Inner Shoulder Joints,” in *Humanoids*, Cancun, Mexico, 2016, pp. 523–529.
[18] PTC, “Creo manikin extension datasheet.” [Online]. Available: http://www.ptc.com/cad/3d-design/ergonomics-human-factors
[19] D. A. Winter, *Biomechanics and Motor Control of Human Movement*. John Wiley & Sons, 2009.
[20] C. Mandery *et al.*, “Unifying Representations and Large-Scale Whole-Body Motion Databases for Studying Human Motion,” *IEEE Transactions on Robotics*, vol. 32, no. 4, pp. 796–809, Aug 2016.